Light-Cone Parton Distribution Functions from Lattice QCD

Constantia Alexandrou,[1,2] Krzysztof Cichy,[3] Martha Constantinou,[4] Karl Jansen,[5]
Aurora Scapellato,[1,6] and Fernanda Steffens[7]

[1]*Department of Physics, University of Cyprus, P.O. Box 20537, 1678 Nicosia, Cyprus*
[2]*Computation-based Science and Technology Research Center, The Cyprus Institute, 20 Kavafi Street, Nicosia 2121, Cyprus*
[3]*Faculty of Physics, Adam Mickiewicz University, Umultowska 85, 61-614 Poznań, Poland*
[4]*Department of Physics, Temple University, Philadelphia, Pennsylvania 19122-1801, USA*
[5]*NIC, DESY, Platanenallee 6, D-15738 Zeuthen, Germany*
[6]*University of Wuppertal, Gaußstrasse 20, 42119 Wuppertal, Germany*
[7]*Institut für Strahlen- und Kernphysik, Rheinische Friedrich-Wilhelms-Universität Bonn, Nussallee 14-16, 53115 Bonn, Germany*

(Received 16 March 2018; published 12 September 2018)

We extract parton distribution functions (PDFs) of the nucleon from lattice QCD using an ensemble of gauge field configurations simulated with light quark masses fixed to their physical values. Theoretical and algorithmic improvements that allow such a calculation include momentum smearing to reach large nucleon boosts with reduced statistical errors, nonperturbative renormalization, target mass corrections, and a novel modified matching of lattice QCD results to connect to what is extracted from experimental measurements. We give results on the unpolarized and helicity PDFs in the modified minimal subtraction scheme at a scale of 2 GeV and reproduce the main features of the experimentally determined quantities, showing an overlap for a range of Bjorken-x values. This first direct nonperturbative evaluation opens a most promising path to compute PDFs in an *ab initio* way on the lattice and provides a framework for investigating also a wider class of similar quantities, which require the evaluation of hadronic matrix elements of nonlocal operators.

DOI: 10.1103/PhysRevLett.121.112001

Introduction.—A key ingredient of our understanding of fundamental particle interactions in the standard model is the *ab initio* evaluation of quantum chromodynamics (QCD) as our theory of the strong interaction between quarks and gluons. A sound and detailed knowledge of the theoretical predictions from QCD will shed light on the early and the present universe and can address open questions in nuclear and particle physics, such as the emergence of protons and other hadrons from the underlying microscopic system of quarks and gluons. In addition, such QCD predictions can provide hints for physics beyond the standard model through precision calculations of appropriate hadronic matrix elements.

Experimentally, a detailed insight into the most inner structure of hadrons is provided by deep inelastic scattering (DIS), which constitutes a most powerful approach to probe the properties of individual quarks and gluons, such as their momentum, spin, and angular momentum. On the theoretical side, parton distribution functions (PDFs), introduced in the 1960s, can be extracted from such DIS experiments through phenomenological analyses. In this way, detailed information about the distribution of, e.g., momentum and spin of quarks and gluons inside hadrons can be obtained. More concretely, within the *parton model*, unpolarized PDFs describe the probability densities of finding a parton with a longitudinal momentum fraction x $(0 \leq x \leq 1)$ of the total momentum of the parent hadron. In fact, a rich experimental program at major facilities, e.g., Brookhaven National Laboratory, CERN, Deutsches Elektronen-Synchrotron, Fermilab, JLab, and SLAC, has provided a wealth of measurements with a corresponding worldwide theoretical effort to interpret the results. In addition, PDFs serve as an essential and indispensable input for collider experiments, such as the LHC.

However, PDFs are still not precisely determined, since one needs a rather large number of different processes and targets and a sophisticated setup for polarized beams and targets for the case of polarized PDFs. In general, one resorts to fits of experimental data aided by phenomenologically motivated *Ansäätze* (see, e.g., Ref. [1]). In addition, knowledge of PDFs only from phenomenological fits cannot be considered as a direct and *ab initio* QCD prediction, as the analysis procedure is not unique [2]. Finally, there are also limitations in accessing the very small x region [3–5].

On the other hand, PDFs are universal and process-independent quantities and are inherently of a nonperturbative nature. Hence, they would be, in principle, a very suitable target for lattice QCD (LQCD) calculations, since LQCD provides a well-defined theoretical framework for computing hadronic matrix elements using directly the QCD Lagrangian. Indeed, there have been very remarkable recent successes of LQCD, such as the precise measurement of the low-lying hadron spectrum including the mass splitting between proton and neutron [6] and the decomposition of the proton spin [7]. However, an LQCD computation of the full x dependence of PDFs related to bilocal operators on the light cone was thought to be impossible for a very long time. Only the lowest moments of PDFs were until recently computed (see, e.g., [8–12]), since these are related to matrix elements of local operators. But, having only very few lowest moments available is clearly insufficient to reconstruct PDFs in a model-independent manner.

In the seminal work by X. Ji [13], a new promising approach [14] to compute PDFs within LQCD was proposed. However, applicability of this approach requires the validation of and control on a number of nontrivial steps, which are to reach large enough nucleon boosts, nonperturbative renormalization, target mass corrections, and a suitable matching. In this Letter, we implement Ji's approach and examine for the first time *all* these steps and successfully determine the unpolarized and polarized PDFs of the proton within LQCD using an ensemble of gauge field configurations simulated with light quarks of physical masses, which is essential for reliable results for these quantities.

Ji's approach to access PDFs proceeds via the computation of spatial correlation functions between two boosted nucleon states, using nonlocal fermionic operators connected with a finite-length Wilson line (WL). Taking the Fourier transform of these matrix elements, it leads to the so-called quasi-PDFs. For large nucleon momenta, contact with light-cone PDFs is reestablished via a matching procedure [19–23]. This approach has been explored in LQCD with promising first results [24–27]. Many aspects of extracting light-cone PDFs from quasi-PDFs have improved recently. These include investigations of renormalizability [28,29], development of a renormalization scheme for lattice WL operators [30], refining the matching procedure [21–23], and target mass corrections [26], which settled initial reservations on the reliability of the quasi-PDF approach. Other related approaches were also proposed and tested [31–35].

Quasi-PDFs.—The Minkowski definition of PDFs within a hadron can be derived from the operator product expansion of hadronic DIS and is light-cone dominated, which makes it impossible to evaluate on a Euclidean lattice. Quasi-PDFs, on the other hand, can be computed in LQCD. They are given by

$$\tilde{q}(x,\Lambda,P) = \int_{-\infty}^{+\infty} \frac{dz}{4\pi} e^{-ixP_3 z} h_\Gamma(P,z), \qquad (1)$$

where $h_\Gamma(P,z) = \langle P|\bar{\psi}(0,z)\Gamma W(z)\psi(0,0)|P\rangle$, $\Lambda \sim 1/a$ is a UV cutoff, $|P\rangle$ is the proton state with finite momentum P, whose spatial components are nonzero only in the direction of the WL $[P = (P_0, 0, 0, P_3)]$. z is the length of the WL between quark fields $[W(z)]$, which is taken in a purely spatial direction instead of the $+$ direction on the light cone. The Dirac structure Γ defines the type of PDF ($\Gamma = \gamma_\mu$—unpolarized, $\Gamma = \gamma_5\gamma_\mu$—polarized, and $\Gamma = \sigma_{\mu\nu}$—transversity) and may be taken parallel or perpendicular to the WL to avoid finite mixing (for certain lattice discretizations) with other operators [36]. To account for the finite momentum used in lattice QCD simulations, higher-twist corrections and target mass corrections need to be applied. For large nucleon momenta, quasi-PDFs can be matched to physical PDFs using the Large Momentum Effective Theory (LMET) [13,37].

Lattice QCD evaluation.—One of the important steps in extracting PDFs is to use simulations with up and down quarks having physical mass. For our calculation we use an ensemble of two degenerate light quarks ($N_f = 2$) with quark masses that are tuned to reproduce approximately the physical pion mass value [38]. The values of parameters of the ensemble are given in Table I. The gauge configurations have been generated with the Iwasaki improved gluon action [39,40] and the twisted mass fermion action (at maximal twist) with clover improvement [41,42].

A crucial step for the applicability of the method is to boost the nucleon to large enough momentum, so one can carry out the matching within perturbation theory. However, the noise-to-signal ratio increases rapidly as the momentum is increased, demanding a corresponding increase in computational effort in order to reach a satisfactory statistical accuracy. One uses momentum smearing to reduce the noise. There are additional factors that contribute to the increase of gauge noise, such as simulating at the physical pion mass, as well as how large the Euclidean time separation needs to be from the time of creating a state with the quantum numbers of the nucleon to annihilating it. We refer to the Euclidean time separation as source-sink separation $T_{\rm sink}$, and this needs to be large enough to sufficiently suppress excited states. We investigate when ground state dominance sets in by employing three values of $T_{\rm sink}$, namely, 0.75, 0.93, and 1.12 fm. We find that the results for $T_{\rm sink} = 0.93$ fm are in agreement

TABLE I. Simulation parameters of the ensemble used in this Letter. The nucleon mass (m_N), the pion mass (m_π), and the lattice spacing (a) have been determined in Ref. [43]. L is the spatial length of the lattice, β is related to the bare coupling constant, and $c_{\rm SW}$ is the clover parameter.

$\beta = 2.10$	$c_{\rm SW} = 1.57751$	$a = 0.0938(3)(2)$ fm
$48^3 \times 96$	$a\mu = 0.0009$	$m_N = 0.932(4)$ GeV
$L = 4.5$ fm	$m_\pi = 0.1304(4)$ GeV	$m_\pi L = 2.98(1)$

with those obtained for $T_{\rm sink} = 1.12$ fm, but not with those for $T_{\rm sink} = 0.75$ fm, and thus excited states are indeed sufficiently suppressed for this larger $T_{\rm sink}$, for which we quote our results in what follows.

Quasi-PDFs are computed for three values of the momentum, namely, $6\pi/L$, $8\pi/L$, and $10\pi/L$, or in physical units 0.83, 1.11, and 1.38 GeV. We use momentum smearing on the nucleon interpolating field [44], which is necessary to achieve high momentum at a reasonable computational cost [27]. Although this means that we need to compute the quark propagator for each value of the momentum, the gain in the error overcompensates by far the extra cost. Going to even larger momentum, although desirable, requires huge computational resources [44,45], beyond what is currently available.

We apply stout smearing [46] to the links of the WL entering the operator. This reduces the power divergence connected to the nonlocal operator modifying the renormalization factor. However, renormalized matrix elements extracted from different smearing levels must agree. We test up to 20 stout smearing steps to the WL (only in spatial directions), and upon renormalization we find complete agreement (see Supplemental Material [47]).

One can extract the unpolarized PDF from an operator with a Dirac structure parallel (h_{γ_3}) or perpendicular to the WL (h_{γ_0}). The former has the disadvantage of mixing with the twist-3 scalar operator [36], and, thus, here we focus on h_{γ_0}. In Fig. 1 we show results for bare unpolarized and helicity matrix elements. It is evident that the signal quality rapidly worsens for larger momenta. To keep statistical uncertainties under control, we increase statistics by a factor of four to six for momenta $8\pi/L$ and $10\pi/L$, where 38 250 and 58 950 measurements are used, respectively, as compared to 9600 measurements for $6\pi/L$. As can be seen from Fig. 1, results for the two largest momenta overlap for both the real and imaginary parts within our statistical errors, demonstrating encouraging convergence.

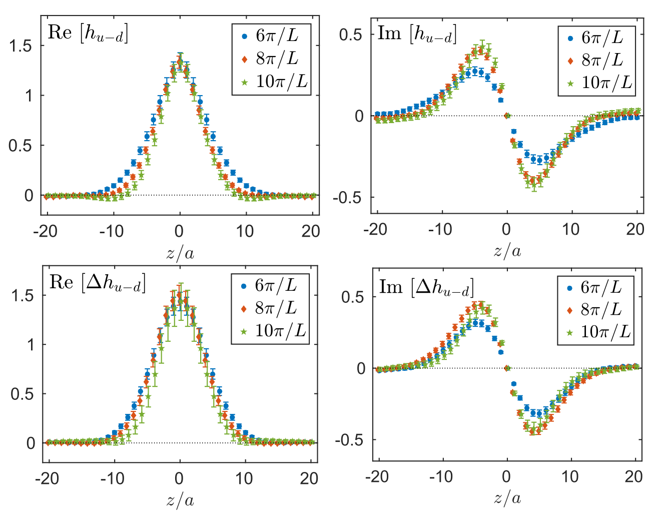

FIG. 1. Comparison of unpolarized (upper panel) and polarized (lower panel) bare matrix elements for momenta $6\pi/L$ (blue circles), $8\pi/L$ (red diamonds), and $10\pi/L$ (green stars) using five stout steps.

Renormalization and matching procedures.—To obtain physical results, lattice matrix elements of nonconserved currents must be renormalized. Compared to other nucleon quantities, quasi-PDFs have an additional WL-related power divergence. Based on the renormalization and mixing pattern from Ref. [36], we developed a nonperturbative prescription [30] (see Supplementary Material [47]), that was also implemented for another lattice formulation [54]. This procedure removes the power divergence and the logarithmic divergence with respect to the regulator and applies the necessary finite renormalization related to the lattice regularization. For our choices of the Dirac structures, there is no mixing. Results are converted to the modified minimal subtraction scheme and evolved to $\mu = 2$ GeV using the formulas of Ref. [36].

Quasi-PDFs are extracted from the renormalized matrix elements by taking a Fourier transform. To obtain the light-cone PDF from quasi-PDF, one needs to apply a perturbative matching procedure [19–23,25], which is valid because infrared physics is the same for both quasi and light-cone PDFs. The matching formula can be expressed as

$$q(x,\mu) = \int_{-\infty}^{\infty} \frac{d\xi}{|\xi|} C\left(\xi, \frac{\mu}{xP_3}\right) \tilde{q}\left(\frac{x}{\xi}, \mu, P_3\right), \qquad (2)$$

where $\tilde{q}(x,\mu,P_3)$ is the renormalized quasi-PDF and $q(x,\mu)$ is the light-cone (matched) renormalized PDF. The negative-x region corresponds to antiquarks, with the crossing symmetry being $\bar{q}(x) = -q(-x)$ (unpolarized) and $\Delta\bar{q}(x) = \Delta q(-x)$ (polarized). C represents the matching kernel (see Supplemental Material [47]), where we use a modified expression with respect to the one suggested in Ref. [23]. More details on the matching and its comparison with other studies [21–23] will be presented in a follow-up publication.

Results.—After applying the matching procedure and target mass corrections [26] to the renormalized Fourier-transformed matrix elements, one can make contact with light-cone PDFs. In Fig. 2, we show results for the unpolarized PDF (h_{γ_0}) for the three different values of the nucleon boost. For illustrative purposes we include the phenomenological determinations CJ15 [55], ABMP16 [56], and NNPDF3.1 [57]. We find that as the momentum increases, the LQCD data approach the phenomenological results. In particular, increasing P_3 from $6\pi/L$ to $8\pi/L$ has a large effect on the shape of the PDFs, with the results obtained at the larger value approaching the phenomenological curves. Furthermore, we find agreement between the PDFs obtained for the two largest boosts indicating that LaMET may be applicable for $P_3 \geq 8\pi/L$. We note that observing such convergence is necessary for reliable

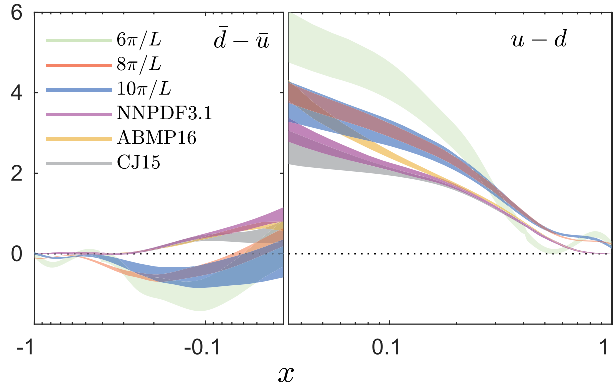

FIG. 2. Comparison of unpolarized PDF at momenta $6\pi/L$ (green band), $8\pi/L$ (red band), and $10\pi/L$ (blue band). The results from the phenomenological analysis of ABMP16 [56] (NNLO), NNPDF [57] (NNLO), and CJ15 [55] (NLO) are displayed for illustrative purposes. Logarithmic scale is used in the x axis (down to $|x| = 0.035$) for better visibility.

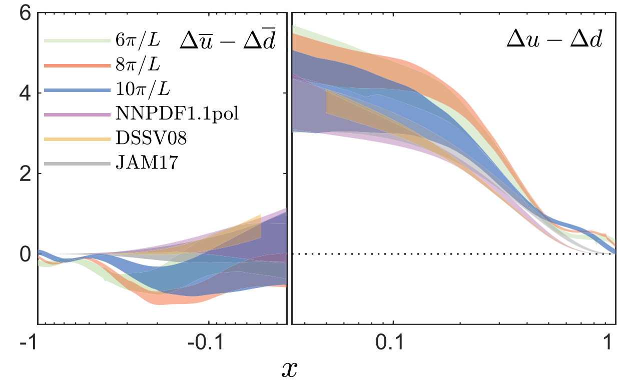

FIG. 3. Comparison of polarized PDF at momenta $6\pi/L$ (green band), $8\pi/L$ (red band), and $10\pi/L$ (blue band), DSSV08 [58], NNPDF1.1pol [59], and JAM17 NLO phenomenological data [60]. Logarithmic scale is used in the x axis (down to $|x| = 0.035$) for better visibility.

results, since there is no known functional form for the P_3 dependence for the infinite momentum limit extrapolation.

The interplay between real and imaginary parts of renormalized matrix elements leads to unphysical oscillations in quasi-PDFs, resulting from the periodicity of the Fourier transform, and propagated through the matching procedure to light-cone PDFs. The effect is naturally suppressed for large nucleon boosts, when matrix elements decay to zero fast enough, before the term e^{-ixP_3z} of Eq. (1) can lead to negative results. For the currently attained momenta, the decay of renormalized matrix elements is still relatively slow, which manifests itself in distorting the approach of the PDFs to zero for $x \gtrsim 0.5$ and in reaching an unphysical minimum in the antiquark part, for $x \approx -0.2$. The oscillations, as expected, are smoothened out as the momentum increases (which is visible particularly at the level of quasi-PDFs) and are more severe in the antiquark region. Nevertheless, this is the first time when clear convergence towards phenomenological PDFs (and partly even agreement with them) is demonstrated with simulations using a physical pion mass value. Clearly, momentum $6\pi/L$ is not high enough to reconstruct light-cone PDFs. However, we do observe a qualitatively similar behavior between the LQCD data at the largest momentum and the phenomenological results, with some overlap in the small-x region. The slope of the two curves is compatible for the positive-x region, and both curves go to zero for $x \lesssim -0.4$ and $x \gtrsim 1$.

In Fig. 3, we present the polarized PDFs for our three values of the momentum, together with DSSV08 [58], NNPDF1.1pol [59], and JAM17 [60] data. We find a milder dependence on the nucleon momentum, and, for the third largest momentum, the results are closer to phenomenological curves with significant overlap with them for $0 < x < 0.5$. For the region $0.5 < x < 1$, the slope of the lattice QCD curves changes, possibly due to the oscillations mentioned above, but they still approach zero around $x = 1$. For the negative-x region, the lattice QCD curves also approach zero, with a dip at small x and large uncertainties, which is another consequence of oscillations. Given that the lattice QCD results are extracted without any assumptions on the functional form, unlike what is done in phenomenological fits, this qualitative agreement is very promising. We note that after eliminating the problem of oscillations and addressing possible higher-twist contamination, the large-x region is expected to be the most reliable, since the access to the very small-x region is limited by the lattice size.

Finally, we discuss the role of having simulations with physical pions. In Fig. 4, we compare phenomenological curves with results from Ref. [27] obtained using an ensemble with $m_\pi \approx 375$ MeV and volume $32^3 \times 64$, referred to as the B55 ensemble. As P_3 increases, the results from this ensemble reach a universal curve. However, they are clearly different from the phenomenological curves. When we compare the curves from the B55 ensemble to those obtained using the ensemble of this Letter, both at momentum ~1.4 GeV, we observe a clear pion mass dependence. This is compatible with the pion mass dependence seen in the isovector quark momentum fraction $\langle x\rangle_{u-d}$ computed within LQCD. For ensembles at heavier than physical pion masses, $\langle x\rangle_{u-d}$ is larger [61], which corresponds to a shift of the curve of the PDF to larger values of x, as indeed observed in the B55 data.

Conclusions and prospects.—In this Letter, we extracted PDFs from lattice QCD simulations, a task that was considered one of the most important aims of lattice hadron structure computations and yet practically unfeasible only a few years ago. The steps addressed in order to achieve this task comprise significant conceptual developments, such as nonperturbative renormalization, target mass corrections, matching, and the development of a lattice technique, momentum smearing, that enables computations for large

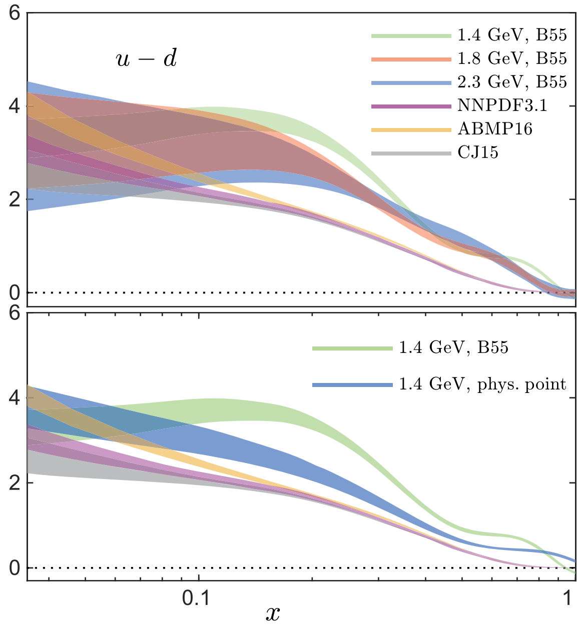

FIG. 4. Upper panel: Comparison of unpolarized PDF from the B55 ensemble and phenomenological determinations. Lower panel: Unpolarized PDF using the ensemble of this Letter (blue) and from the B55 ensemble (orange) at momentum ∼1.4 GeV.

nucleon boosts. An essential step in our work was to simulate with light quark masses corresponding to the physical pion mass, which needed a tremendous simulation effort of our whole ETM Collaboration [38,61] and large amounts of supercomputing power. Applying all these nontrivial steps allowed us to evaluate for the first time the polarized and unpolarized PDFs from first principles, directly from the QCD Lagrangian.

A number of challenges still remain. Even with our optimized interpolating fields, going from a momentum of 0.83 to 1.38 GeV requires a significant increase in the number of measurements to keep statistical uncertainties under control and at the same time ensure ground state dominance. Reaching larger momenta without compromising the reliability of results will allow us to check the size of higher-twist effects and treat the problem of unphysical oscillations. The present calculation was done using a single ensemble, and thus finite lattice spacing effects were not examined. Although a study using ensembles simulated with larger than physical pion mass shows a weak dependence for similar values of the momentum, taking the continuum limit will require large-scale computations for at least two additional ensembles with smaller lattice spacings and corresponding larger lattice volumes. As discussed in Ref. [62] for models including scalar particles that are analogous to pion and nucleon QCD, finite volume effects could be non-negligible. Therefore, a larger physical volume is desirable. Finite lattice effects could be sizable in the renormalization functions. Estimating these effects to order $\mathcal{O}(g^2a^\infty)$ perturbatively, as done for the local operators [63], is expected to also improve their determination here. In addition, investigation of perturbative truncation effects present in the matching and conversion to the modified minimal subtraction scheme, with a two-loop computation, is highly desirable.

Despite these remaining challenges that need to be addressed in the future, our work validates the methodology of Ji's proposal. Our final results for PDFs highlighted in Figs. 2–3 can for the first time be compared meaningfully with the phenomenologically extracted PDFs as all necessary steps to determine the PDFs from lattice data have been applied. The comparison still remains qualitative before addressing the systematic effects described above, but there are already features in our results indicating that in the future, the approach will lead to accurate *ab initio* determinations of PDFs from lattice simulations.

We conclude by emphasizing that the lattice QCD extraction of PDFs proceeds without any input or assumption on their functional form. This is a major breakthrough that paves the way for the prediction of, e.g., transversity PDFs, for which currently the uncertainties are much larger [64,65] than the deviations observed between the LQCD-determined helicity PDF and the PDF from global analysis of experimental data. The approach can also be applied to other hadrons [66] and can be extended to other quantities. Examples of those are generalized parton distributions and transverse-momentum dependent PDFs (TMDs), which probe how partons are distributed in the plane transverse to the direction in which the proton is moving.

We would like to thank all members of ETMC for their constant and pleasant collaboration. M. C. is thankful to Zein-Eddine Meziani for the many fruitful and inspiring discussions. We also thank the CJ, ABMP, and NNPDF Collaborations for providing their phenomenological parametrizations. This work has received funding from the European Union's Horizon 2020 research and innovation program under Marie Skłodowska-Curie Grant Agreement No. 642069 (HPC-LEAP). K. C. was supported by National Science Centre (Poland) Grant SONATA BIS No. 2016/22/E/ST2/00013. F. S. was funded by DFG Project No. 392578569. M. C. acknowledges financial support by the U.S. Department of Energy, Office of Nuclear Physics, within the framework of the TMD Topical Collaboration, as well as by the National Science Foundation under Grant No. PHY-1714407. This research used resources of the Oak Ridge Leadership Computing Facility, which is a DOE Office of Science User Facility supported under Contract No. DE-AC05-00OR22725, the Prometheus supercomputer at the Academic Computing Centre Cyfronet AGH in Cracow (grant ID *quasipdfs*), the Eagle supercomputer at the Poznan Supercomputing and Networking Center (Grant No. 346), and the Okeanos supercomputer at the Interdisciplinary Centre for Mathematical and Computational Modelling in Warsaw (Grant IDs gb70-17 and ga71-22).

[1] H.-W. Lin *et al.* Prog. Part. Nucl. Phys. **100**, 107 (2018).
[2] P. Jimenez-Delgado, W. Melnitchouk, and J. F. Owens, J. Phys. G **40**, 093102 (2013).
[3] L. V. Gribov, E. M. Levin, and M. G. Ryskin, Phys. Rep. **100**, 1 (1983).
[4] A. H. Mueller and J.-W. Qiu, Nucl. Phys. **B268**, 427 (1986).
[5] L. D. McLerran and R. Venugopalan, Phys. Rev. D **49**, 2233 (1994).
[6] S. Borsanyi *et al.*, Science **347**, 1452 (2015).
[7] C. Alexandrou, M. Constantinou, K. Hadjiyiannakou, K. Jansen, C. Kallidonis, G. Koutsou, A. V. Avils-Casco, and C. Wiese, Phys. Rev. Lett. **119**, 142002 (2017).
[8] M. Constantinou, Proc. Sci., LATTICE20142015 (**2015**) 001.
[9] M. Constantinou, Proc. Sci., CD152015 (**2015**) 009.
[10] C. Alexandrou and K. Jansen, Nucl. Part. Phys. Proc. **261–262**, 202 (2015).
[11] C. Alexandrou, in *Proceedings of the 45th International Symposium on Multiparticle Dynamics, Kreuth, Germany, 2015* (ISMD, 2015), http://arxiv.org/abs/arXiv:1512.03924.
[12] S. Syritsyn, Proc. Sci., LATTICE20132014 (**2014**) 009.
[13] X. Ji, Phys. Rev. Lett. **110**, 262002 (2013).
[14] Other direct approaches proposed over many years include the ones discussed in Refs. [15–18]. They have, however, obtained comparatively much less attention than the quasi-PDF approach.
[15] K.-F. Liu and S.-J. Dong, Phys. Rev. Lett. **72**, 1790 (1994).
[16] U. Aglietti, M. Ciuchini, G. Corbo, E. Franco, G. Martinelli, and L. Silvestrini, Phys. Lett. B **441**, 371 (1998).
[17] W. Detmold and C. J. D. Lin, Phys. Rev. D **73**, 014501 (2006).
[18] V. Braun and D. Mueller, Eur. Phys. J. C **55**, 349 (2008).
[19] X. Xiong, X. Ji, J.-H. Zhang, and Y. Zhao, Phys. Rev. D **90**, 014051 (2014).
[20] J.-W. Chen, X. Ji, and J.-H. Zhang, Nucl. Phys. **B915**, 1 (2017).
[21] W. Wang, S. Zhao, and R. Zhu, Eur. Phys. J. C **78**, 147 (2018).
[22] I. W. Stewart and Y. Zhao, Phys. Rev. D **97**, 054512 (2018).
[23] T. Izubuchi, X. Ji, L. Jin, I. W. Stewart, and Y. Zhao, arXiv:1801.03917v1.
[24] H.-W. Lin, J.-W. Chen, S. D. Cohen, and X. Ji, Phys. Rev. D **91**, 054510 (2015).
[25] C. Alexandrou, K. Cichy, V. Drach, E. Garcia-Ramos, K. Hadjiyiannakou, K. Jansen, F. Steffens, and C. Wiese, Phys. Rev. D **92**, 014502 (2015).
[26] J.-W. Chen, S. D. Cohen, X. Ji, H.-W. Lin, and J.-H. Zhang, Nucl. Phys. **B911**, 246 (2016).
[27] C. Alexandrou, K. Cichy, M. Constantinou, K. Hadjiyiannakou, K. Jansen, F. Steffens, and C. Wiese, Phys. Rev. D **96**, 014513 (2017).
[28] T. Ishikawa, Y.-Q. Ma, J.-W. Qiu, and S. Yoshida, Phys. Rev. D **96**, 094019 (2017).
[29] X. Ji, J.-H. Zhang, and Y. Zhao, Phys. Rev. Lett. **120**, 112001 (2018).
[30] C. Alexandrou, K. Cichy, M. Constantinou, K. Hadjiyiannakou, K. Jansen, H. Panagopoulos, and F. Steffens, Nucl. Phys. **B923**, 394 (2017).
[31] A. Radyushkin, Phys. Lett. B **767**, 314 (2017).
[32] A. Radyushkin, Phys. Lett. B **770**, 514 (2017).
[33] A. V. Radyushkin, Phys. Rev. D **96**, 034025 (2017).
[34] K. Orginos, A. Radyushkin, J. Karpie, and S. Zafeiropoulos, Phys. Rev. D **96**, 094503 (2017).
[35] Y.-Q. Ma and J.-W. Qiu, Phys. Rev. Lett. **120**, 022003 (2018).
[36] M. Constantinou and H. Panagopoulos, Phys. Rev. D **96**, 054506 (2017).
[37] X. Ji, Sci. China Phys. Mech. Astron. **57**, 1407 (2014).
[38] A. Abdel-Rehim *et al.* (ETM Collaboration), Phys. Rev. D **95**, 094515 (2017).
[39] Y. Iwasaki, arXiv:1111.7054.
[40] A. Abdel-Rehim *et al.*, Proc. Sci., LATTICE2013 (**2014**) 264.
[41] R. Frezzotti and G. C. Rossi, J. High Energy Phys. 08 (2004) 007.
[42] B. Sheikholeslami and R. Wohlert, Nucl. Phys. **B259**, 572 (1985).
[43] C. Alexandrou and C. Kallidonis, Phys. Rev. D **96**, 034511 (2017).
[44] G. S. Bali, B. Lang, B. U. Musch, and A. Schäfer, Phys. Rev. D **93**, 094515 (2016).
[45] B. Yoon, M. Engelhardt, R. Gupta, T. Bhattacharya, J. R. Green, B. U. Musch, J. W. Negele, A. V. Pochinsky, A. Schäfer, and S. N. Syritsyn, Phys. Rev. D **96**, 094508 (2017).
[46] C. Morningstar and M. J. Peardon, Phys. Rev. D **69**, 054501 (2004).
[47] See Supplemental Material at http://link.aps.org/supplemental/10.1103/PhysRevLett.121.112001 for details on the calculation of the matrix elements, renormalization, and matching procedures, which includes Refs. [48–53].
[48] S. Gusken, Nucl. Phys. B, Proc. Suppl. **17**, 361 (1990).
[49] C. Alexandrou, S. Gusken, F. Jegerlehner, K. Schilling, and R. Sommer, Nucl. Phys. **B414**, 815 (1994).
[50] M. Albanese *et al.* (APE Collaboration), Phys. Lett. B **192**, 163 (1987).
[51] C. Alexandrou, S. Bacchio, K. Cichy, M. Constantinou, K. Hadjiyiannakou, K. Jansen, G. Koutsou, A. Scapellato, and F. Steffens, EPJ Web Conf. **175**, 14008 (2018).
[52] T. Blum, T. Izubuchi, and E. Shintani, Phys. Rev. D **88**, 094503 (2013).
[53] G. Martinelli, C. Pittori, C. T. Sachrajda, M. Testa, and A. Vladikas, Nucl. Phys. **B445**, 81 (1995).
[54] J.-W. Chen, T. Ishikawa, L. Jin, H.-W. Lin, Y.-B. Yang, J.-H. Zhang, and Y. Zhao, Phys. Rev. D **97**, 014505 (2018).
[55] A. Accardi, L. T. Brady, W. Melnitchouk, J. F. Owens, and N. Sato, Phys. Rev. D **93**, 114017 (2016).
[56] S. Alekhin, J. Blumlein, S. Moch, and R. Placakyte, Phys. Rev. D **96**, 014011 (2017).
[57] R. D. Ball *et al.* (NNPDF Collaboration), Eur. Phys. J. C **77**, 663 (2017).
[58] D. de Florian, R. Sassot, M. Stratmann, and W. Vogelsang, Phys. Rev. D **80**, 034030 (2009).
[59] E. R. Nocera, R. D. Ball, S. Forte, G. Ridolfi, and J. Rojo (NNPDF Collaboration), Nucl. Phys. **B887**, 276 (2014).
[60] J. J. Ethier, N. Sato, and W. Melnitchouk, Phys. Rev. Lett. **119**, 132001 (2017).

[61] A. Abdel-Rehim *et al.*, Phys. Rev. D **92**, 114513 (2015); **93**, 039904(E) (2016).
[62] R. A. Briceño, J. V. Guerrero, M. T. Hansen, and C. J. Monahan, Phys. Rev. D **98**, 014511 (2018).
[63] C. Alexandrou, M. Constantinou, and H. Panagopoulos (ETM Collaboration), Phys. Rev. D **95**, 034505 (2017).
[64] H.-W. Lin, W. Melnitchouk, A. Prokudin, N. Sato, and H. Shows, Phys. Rev. Lett. **120**, 152502 (2018).
[65] M. Radici and A. Bacchetta, Phys. Rev. Lett. **120**, 192001 (2018).
[66] J.-W. Chen, L. Jin, H.-W. Lin, Y.-S. Liu, A. Schäfer, Y.-B. Yang, J.-H. Zhang, and Y. Zhao, arXiv:1804.01483.